

1 **Variability in terrigenous sediment supply offshore of the Rio de la Plata (Uruguay)**
2 **recording the continental climatic history over the past 1200 years**

3
4 L. Perez^{1,4*}, F. García-Rodríguez^{1,4}, T. J. J. Hanebuth^{2,3}

5 ¹ Sección Oceanología, Facultad de Ciencias, Universidad de la República, Iguá 4225,
6 Montevideo 11400 (Uruguay).

7 ² School of Coastal and Marine Systems Sciences, Coastal Carolina University, SC 29528
8 (USA).

9 ³ MARUM – Center for Marine Environmental Sciences, University of Bremen, Leobener
10 Straße, 28359 Bremen (Germany).

11 ⁴ Centro Universitario Regional Este, CURE-Rocha, Ruta 9 intersección Ruta 15, Rocha
12 (Uruguay).

13 Correspondence to: L. Perez (lp3_3@hotmail.com)

14

15

16 **Abstract**

17 The continental shelf adjacent to the Río de la Plata (RdIP) exhibits extremely complex
18 hydrographic and ecological characteristics which are of great socio-economic importance. Since
19 the long-term environmental variations related to the atmospheric (wind fields), hydrologic
20 (freshwater plume), and oceanographic (currents and fronts) regimes are little known, the aim of
21 this study is to reconstruct the changes in the terrigenous input into the inner continental shelf
22 during the Late Holocene period (associated with the RdIP sediment discharge) and to unravel
23 the climatic forcing mechanisms behind them. To achieve this, we retrieved a 10-m long
24 sediment core from the RdIP mud depocenter at 57 m water depth (GeoB 13813-4). The
25 radiocarbon age control indicated an extremely high sedimentation rate of 0,8 cm per year,
26 encompassing the past 1200 years (750-2000 AD). We used element ratios (Ti/Ca, Fe/Ca, Ti/Al,
27 Fe/K) as regional proxies for the fluvial input signal, and the variations in relative abundance of
28 salinity-indicative diatom groups (freshwater versus marine-brackish), to assess the variability in
29 terrigenous freshwater and sediment discharges. Ti/Ca, Fe/Ca, Ti/Al, Fe/K and the freshwater
30 diatom group showed the lowest values between 850 and 1300 AD, while the highest values
31 occurred between 1300 and 1850 AD.

32 The variations in the sedimentary record can be attributed to the Medieval Climatic Anomaly
33 (MCA) and the Little Ice Age (LIA), both of which had a significant impact on rainfall and wind
34 patterns over the region. During the MCA, a northward migration of the Intertropical
35 Convergence Zone (ITCZ), and an associated weakening of the South American Summer
36 Monsoon System (SAMS) and the South Atlantic Convergence Zone (SACZ), could explain the
37 lowest element ratios (indicative of a lower terrigenous input) and a marine-dominated diatom
38 record, both indicative of a reduced RdIP freshwater plume. In contrast during the LIA, the
39 southward migration of the ITCZ, and a strengthening of SAMS and SACZ, may have led to an
40 expansion of the RdIP river plume to the far north, as indicated by higher element ratios and a
41 marked freshwater diatom signal. Furthermore, a possible multi-decadal oscillation probably
42 associated with Atlantic Multidecadal Oscillation (AMO) since 1300 AD, reflects the variability
43 in both the SAMS and SACZ systems.

44 **Keywords**

45 Terrigenous sediment supply, element ratios, salinity-indicative diatom groups, historical
46 climatic changes, Intertropical Convergence Zone, South American Summer Monsoon System,
47 South Atlantic Convergence Zone, Río de la Plata, mud depocenter, continental shelf, Uruguay.

48 **1 Introduction**

49 The Río de la Plata (RdIP) estuary is fed by the Paraná and the Uruguay Rivers and drains into
50 the Southwestern Atlantic Ocean (SWAO) forming the second largest estuary system in South
51 America (Bisbal, 1995; Acha et al., 2003). The RdIP is the main source of continental freshwater
52 and sediments entering the SWAO (Piola et al., 2008; Krastel et al., 2011, 2012; Razik et al.,
53 2013; Lantzsch et al., 2014; Nagai et al., 2014). In this sense, the RdIP provides an average
54 annual suspended sediment load of 79.8×10^6 tons yr^{-1} (Depetris et al., 2003). Most of this
55 discharge is directed close to the Uruguayan coast towards the inner continental shelf (Depetris
56 et al., 2003; Gilberto et al., 2004). The RdIP freshwater discharge, leads to a low salinity plume
57 on the inner continental shelf, which can reach northerly areas up to 28°S (Piola et al. 2000). The
58 low-salinity waters on the inner part of the continental shelf extend downwards to a depth of
59 approximately 50 m, while the outer part of the continental shelf (from 50 m to 200 m) is
60 influenced by the Subtropical Confluence, where the warm, salty southward-flowing Brazil
61 Current collides with the cold and less salty northward-flowing Malvinas Current (Piola et al.,
62 2000).

63 The Paraná River contributes about 73% to the total RdIP freshwater discharge and maximum
64 values are found during austral summer (Depetris and Pasquini, 2007). This precipitation and
65 river discharge pattern is associated with the southward expansion and intensification of the
66 South American Summer Monsoon System (SAMS; Zhou and Lau, 1998; Chiessi et al., 2009).
67 The SAMS is known to be a poleward displacement of the Intertropical Convergence Zone
68 (ITCZ), and it is associated with a wet season that begins in the equatorial Amazon and
69 propagates rapidly eastward and southeastward during austral spring (García and Kayano, 2010).
70 The SAMS is tightly associated with the South Atlantic Convergence Zone (SACZ, Carvalho et
71 al., 2004), which is a main component of the SAMS (Nogués-Paegle et al., 2002; Almeida et al.,
72 2007). The SACZ is an elongated NW-SE band of convective activity that originates in the
73 Amazon Basin, which extends above the northern RdIP drainage basin, and has its southernmost

74 limit in the adjacent SWAO (Carvalho et al., 2004). Thus, the Paraná River discharge is largely
75 determined by the SACZ (Robertson and Mechoso, 2000).

76 The RdIP is an extremely dynamic system which exhibits complex hydrodynamic features
77 associated with the climatic pattern that affect the wind and oceanographic systems, as well as
78 the river discharge (Piola et al., 2008). As mentioned above, a natural intra-annual variability
79 exists with a higher river discharge during the summer season (Depetris and Pasquini, 2007).
80 Besides, a northerly wind pattern during summer leads to a southward and offshore displacement
81 of the low-salinity RdIP freshwater plume (Guerrero et al., 1997; Möller et al., 2008; Piola et al.,
82 2008). In contrast during the winter season, existed a lower RdIP discharge, but exists a
83 predominant southerly wind pattern (associated with a northward displacement of the
84 Westerlies). This situation forces a northward displacement of the RdIP plume and thus,
85 considerably diminishes the salinity on the southern Brazilian continental shelf (Guerrero et al.,
86 1997; Camilloni, 2005; Möller et al., 2008; Piola et al., 2008).

87 The regional climatic system also exhibits an inter-annual and inter-decadal variability,
88 associated with environmental changes (expressed mainly in precipitation patterns) related to the
89 El Niño/La Niña Southern Oscillation (ENSO) and the Pacific Decadal Oscillation (PDO),
90 respectively (Depetris and Kempe, 1990; Depetris et al., 2003; Depetris and Pasquini, 2007;
91 Garreaud et al., 2009; Barreiro, 2010). PDO is associated with ENSO as both seem to produce
92 similar climatic effects, though their mechanisms are not yet fully understood (Garreaud et al.,
93 2009). In this sense, it has been suggested that during both the warm El Niño and the positive
94 PDO phases, there is an increasing trend in precipitations over the RdIP drainage basin
95 associated with an intensification of the SAMS, which leads to a higher RdIP river discharge,
96 while the opposite trend was observed for the negative phases (Ciotti et al., 1995; Depetris and
97 Pasquini, 2007; Garreaud et al., 2009; Barreiro, 2010; García-Rodríguez et al., 2014). However,
98 Piola et al (2005) reported strong NE winds during El Niño conditions which compensate the
99 effect of the positive precipitation anomalies, and thus prevent an anomalous northeastward
100 displacement of the RdIP plume. In addition, there is evidence that the interannual variability in
101 the RdIP drainage basin has a stronger influence on the Uruguay River discharge, whilst the
102 decadal variability is most pronounced in the Paraná River supply (Robertson and Mechoso,
103 2000). Furthermore, Chiessi et al. (2009) published evidence that the Atlantic Multidecadal

104 Oscillation (AMO) influences SAMS intensity on the multidecadal time scales.

105 Regarding the Late Holocene period, a significant number of studies has described the climatic
106 history of South America over the last 1500 cal yr BP (calibrated thousands of years before
107 present), i.e., for the Medieval Climatic Anomaly (MCA, 800-1300 AD) and the Little Ice Age
108 (LIA, 1400-1800 AD), (Cioccale, 1999; Iriondo, 1999; Piovano et al., 2009; del Puerto et al.,
109 2011; Vuille et al., 2012; del Puerto et al., 2013; Salvatecci et al., 2014). These climatic changes
110 have affected the precipitation pattern over South America with regional differences. For eastern
111 Uruguay, this means a warmer and more humid pulse during the MCA, while in the LIA, a drier
112 and colder climate was recorded (del Puerto et al., 2013). Piovano et al. (2009) have inferred
113 similar climatic conditions for the northeastern region of Argentina. In contrast, the opposite
114 pattern was reported for southern Chile and Argentina, where a dry period occurred during the
115 MCA, and a wetter pulse governed the LIA (Haberzettl et al., 2005). Furthermore, Vuille et al.
116 (2012) inferred similar conditions for southeastern Brazil as Haberzettl et al. (2005).

117 Nevertheless, little is known about how the natural climatic variability over South America
118 affects sedimentation, salinity and river discharge on the continental shelf in front of the RdIP,
119 during the Late Holocene period (Burone et al., 2012; Perez et al., in press). The aim of this
120 study therefore, is to determine the variations in the terrigenous sediment input into the ocean
121 over the last 1200 cal yr BP. To determine how the continental influence competed with the
122 marine regime, a 10-m long sediment core was taken from a confined mud depocenter on the
123 inner Uruguayan continental shelf (GeoB 13813-4, Fig. 1). The sedimentary succession of this
124 core was analyzed for major chemical elements (Ca, Ti, Al, Fe, and K) and compared with
125 previously published data of the diatom salinity-indicative groups, i.e. freshwater (F) and marine,
126 marine-brackish (M-B), (Perez et al. in press) in order to assess variations in continental
127 influence.

128 2 Study Area

129 The study area is located on the Uruguayan inner continental shelf hosting the RdIP mud
130 depocenter (50 m water depth, Fig. 1a, b). This silty clay depocenter (Martins and Urien, 2004;
131 Lantzsch et al., 2014) is the result of regional paleogeographic evolution and is associated with
132 deposits of fluvial origin (Urien and Ewing, 1974). The depocenter built up inside the RdIP

133 paleo-valley which was incised by the Paleo-Paraná River during lower sea levels (Masello and
134 Menafra, 1998; Martins et al., 2003; Lantzsich et al., 2014; Hanebuth et al., in press). The RdIP
135 paleo-valley depression offers an effective protection against the generally strong hydrodynamic
136 conditions on the shelf, thus favoring the deposition and preservation of these muds (Fig. 1b).

137 **3 Materials and Methods**

138 A 1028-cm long sediment core (GeoB 13813-4) was taken from the RdIP mud depocenter
139 (34°44'13" S, 53°33'16" W) during research cruise M76/3a with the German research vessel
140 “Meteor” in July 2009 (Krastel et al., 2012; Fig. 1a). During this expedition, sub-bottom
141 profiling with the shipboard PARASOUND system (4 kHz) showed an elongated depression on the
142 seafloor corresponding to the RdIP paleo-valley filled with a complex pattern of acoustic facies
143 (Fig. 1b, Krastel et al., 2012; Lantzsich et al., 2014).

144 **3.1 Age-depth model and sedimentation rates**

145 Material from bivalve shells collected from six sediment samples, distributed evenly over the
146 core and preserved in life position, were used for radiocarbon dating (^{14}C), (Tab.1). The samples
147 were analyzed using AMS- ^{14}C (accelerated mass spectrometry) at the Poznan Radiocarbon
148 Laboratory in Poland. The age depth model was then generated by using the free software Bacon
149 (Blaauw and Christen, 2011, Fig. 2). The raw ^{14}C dates were calibrated using the calibration
150 curve Marine13 (Reimer et al., 2013, cc=2) integrated into this program, and the weighted
151 average ages are expressed in table 1 (Blaauw and Christen, 2011). **The standard reservoir age of
152 405 years was applied during calibration due to a lack of regional data, although intense water
153 mixing in shallow waters might lead to a significantly smaller reservoir age (Reimer et al. 2013).**

154 Bacon software is an approach for developing an age-depth model that uses Bayesian statistics to
155 reconstruct Bayesian accumulation histories for sedimentary deposits. Bacon divides a sediment
156 core into vertical sections (5 cm thick), and estimates the sedimentation rate (years/cm) for each
157 section through millions of Markov Chain Monte Carlo (MCMC) iterations.

158 **3.2 Paleo-environmental proxies**

159 The two methodological approaches combined in this study were chosen according to previous

160 successful applications for inferring continental versus marine influences in the Atlantic Ocean,
161 (Romero et al., 1999; Chiessi et al., 2009; Mahiques et al., 2009; Govin et al., 2012; Burone et
162 al., 2013; Perez et al., in press), as indicated below.

163 **3.2.1 Runoff-indicative element ratios**

164 The relative concentrations (expressed in counts per second, cps) of the major chemical elements
165 used in this study (Ca, Ti, Fe, K, Al) were obtained by an X-ray fluorescent (XRF) sediment core
166 scanner AVAATECH at MARUM, University of Bremen. XRF core scanning is a fast, non-
167 destructive technique, which allows for the detection of a large number of chemical elements
168 (Löwemark et al., 2011). This technique does not measure absolute element concentrations, but
169 relative intensities. As a consequence, the intensities of the elements are influenced by numerous
170 factors such as water content and sediment density, organic matter content, grain size, biogenic
171 contributions, and carbonate dissolution (Weltje and Tjallingii, 2008). For these reasons, it is
172 unwise to use single element intensities, and it is more appropriate to use element ratios to
173 normalize the data (Weltje and Tjallingii, 2008; Francus et al., 2009; Govin et al., 2012). Core
174 GeoB 13813-4 was scanned in 1-cm steps throughout, and the Ti/Ca, Fe/Ca, Fe/K and Ti/Al
175 element ratios were used.

176 Ti, Fe and Al are elements related to aluminum/silicates, and are associated with clay minerals
177 carried from the continent as weathering products, and through river discharge, they enter into
178 the ocean (Goldberg and Arrhenius, 1958; Jansen et al., 1992; Yarincik et al., 2000). Therefore
179 these elements vary with the terrigenous portion in offshore sediment (Martins et al., 2007;
180 Burone et al., 2013). Most of the K in marine sediments is also associated with terrigenous
181 materials (Goldberg and Arrhenius, 1958), and occurs mainly in fully arid regions where
182 chemical weathering rates are lower (Govin et al., 2009). In contrast, Ca mainly reflects the
183 marine carbonate content in the sediment, and is thus associated with the local marine
184 productivity (Haug et al., 2001; Salazar et al., 2004; Gonzalez-Mora and Sierro, 2007). Al, Ti
185 and K are little affected by biological and redox variations, whilst Fe is sometimes altered by
186 redox processes (Löwemark et al., 2011; Jansen et al., 1992; Yarincik et al., 2000). Burone et al.
187 (2013) recorded a decreasing seaward gradient in Ti, Fe, Al from surface sediment transect from
188 the inner RdIP off to the shelf. In addition, they observed the opposite trend for Ca.

189 Numerous studies used major elements in marine sediments to reconstruct climatic history, but
190 the choice of particular element ratios and the interpretation of such proxies vary from site to site
191 (Govin et al., 2012). Ti/Ca and Fe/Ca ratios were widely used to reconstruct the continental
192 versus the marine influence in the SWAO region (Chiessi et al., 2009; Mahiques et al., 2009;
193 Govin et al., 2012; Bender et al., 2013; Burone et al., 2013). On the other hand, Fe/K and Ti/Al
194 ratio was used in South America to reflect the degree of chemical weathering in areas without
195 significant eolian input (Govin et al., 2012), such as the case of the RdIP (Mahowald et al.,
196 2006). As a consequence of the mentioned above, we used element ratios (Ti/Ca, Fe/Ca, Ti/Al,
197 Fe/K) as regional proxies for the fluvial input signal on the inner Uruguayan continental shelf.

198 3.2.2 Salinity-indicative diatom groups

199 Samples for diatom analyses were first chemically treated (with the aim of cleaning the material
200 from carbonates, organic matter and clay particles) as explain in Perez et al. (in press). Diatom
201 samples were first treated with $\text{Na}_2\text{P}_2\text{O}_7$ to deflocculate the sediment and eliminate clay particles.
202 The samples were then treated with a 35 % HCl to remove inorganic carbonate material. Finally,
203 the samples were boiled in 30 % H_2O_2 for two hours to eliminate organic matter (Metzeltin and
204 García-Rodríguez, 2003). Between each treatment, samples were rinsed at least four times with
205 distilled water. Permanent sediment slides were mounted using the Entellan® mounting medium.
206 A minimum of 400 valves was counted on each slide with a light microscope at 1250 x
207 magnification. The diatoms were then identified and counted at 10 cm depth intervals throughout
208 the sediment core and in 1 cm steps within the uppermost 100 cm. Diatom species were
209 identified and separated into two groups according to their ecological salinity preference, i.e., in
210 groups indicating freshwater (F) and marine/marine-brackish (M-B) conditions, according to
211 Frenguelli (1941, 1945), Müller-Melchers (1945, 1953, 1959), Hasle and Syversten (1996),
212 Witkowski et al. (2000), Metzeltin and García-Rodríguez (2003), Metzeltin et al. (2005), Hassan
213 et al. 2010, Sar et al. (2010) and other standard diatom literature (Perez et al., in press).

214 Romero et al. (1999) determined variations in the continental water discharge by using
215 freshwater diatoms (especially from the genus *Aulacoseira*) along a sediment surface transect
216 from the eastern South Atlantic coast to the open ocean. The same approach was also used in this
217 study to evaluate the freshwater influx on the inner continental shelf.

218 4 Results

219 4.1 Age-depth model and sedimentation rates

220 The core's base was dated to 1200 cal yr BP (750 AD), while a sample at 255 cm was dated to
221 230 cal yr BP (1700 AD, Table 1). The sedimentation rate varied between 0.68 and 1.0 cm yr⁻¹,
222 with a mean sedimentation rate of 0.8 cm yr⁻¹. Minimum values were observed in the top section
223 (i.e., at 200 to 350 cm) and in the bottom section (i.e., at 705 to 967 cm), while the highest values
224 were observed in the middle of the core (at 500 to 705 cm).

225 4.2 Paleo-environmental proxies

226 4.2.1 Runoff-indicative element ratios

227 All the element ratios (Ti/Al, Fe/K, Ti/Ca and Fe/Ca) showed similar profiles (Fig. 3). The
228 lowest values were recorded between 850-1300 AD (coinciding with the MCA), and remained
229 stable during this interval of time. In contrast, high values were recorded from 1300 to 1850 AD
230 (associated with the LIA) and showed a high variability with a number of sharp maxima. In that
231 sense, for the Ti/Al and Fe/K ratios we recorded, a succession of peaks and lows approximately
232 every 100 years (from 1300 to 1500 AD) and every 50 years (1500 AD up to the present), (Fig.
233 3). Moreover during the last century, all element ratios showed a rapid increase toward the
234 highest measured values, most pronounced over the last 50 years (Fig. 3).

235 4.2.2 Salinity-indicative diatom groups

236 Regarding the salinity-indicative diatom groups as shown in Perez et al. (in press), the profile of
237 Group F seems to generally run parallel to those of the four element ratios with lower
238 percentages around 20 % during the MCA times, and higher up to 60 %, rising and more variable
239 values during the LIA period (Fig. 3). An exception is observed for the last 50 yr BP where the
240 percentages declined rapidly towards the former values counted for the MCA time interval. In
241 contrast, the Group M-B ranged from 30 to 80 % generally describing the expected opposite
242 trend compared to the F group (Fig. 3). Over the last 100 yr BP (1900 AD up to the present), an
243 increasing rapid trend coincides with the highest values shown for the element ratios (Fig. 3).

244 5 Interpretation and Discussion

245 5.1 Age-depth model and sedimentation rates

246 The RdIP mud depocenter shows an exceptionally high sedimentation rate (0.8 cm yr^{-1} on
247 average) compared with other records from the southern Brazilian continental shelf (Mahiques et
248 al., 2009; Chiessi et al., 2014). This high sedimentation rate is consequence of the enormous
249 amount of sediment transported by the Paraná and Uruguay Rivers into the RdIP watershed and
250 further onto the Uruguayan shelf (Lantzsch et al., 2014). In addition, an amplification of the
251 sedimentation rate could be a consequence of the fact that the RdIP paleo-valley depression
252 offers protection against strong hydrodynamic conditions on the shelf, favoring the deposition of
253 sediments (Lantzsch et al., 2014; Hanebuth et al., in press). The beginning of sedimentation is
254 possibly associated with the establishment of humidity conditions in the Late Holocene which
255 have resulted in an increasing RdIP River discharge, as well as a significant sedimentation of
256 terrigenous material over the RdIP paleo-valley (Urien et al., 1980; Iriondo, 1999; Mahiques et
257 al., 2009; Lantzsch et al., 2014).

258 5.2 Paleo-environmental proxy records

259 The proxy data used in this study are correlated positively with each other (excluding the last
260 century), and reveal the direct influence of the RdIP as a source of terrigenous sediments within
261 the inner Uruguayan continental shelf.

262 The element ratios Ti/Ca and Fe/ Ca indicates, as do other geochemical and biological proxies
263 (Perez et al., in press), a mixed fluvio-marine signal on the inner Uruguayan continental shelf,
264 spanning over the last 1200 years. Ti and Fe are supplied from the RdIP watershed (Depetris et
265 al., 2003), whilst Ca is an element associated with calcareous organisms such as small mollusks,
266 forams and coccolithophorides in the ocean, and therefore it is related to the marine-biogenic
267 productivity of the continental shelf (Depetris and Pasquini, 2007; Govin et al., 2012; Razik et
268 al., 2013). Thus the variability in these element ratios indicates different degrees of continental
269 influence in the study area during the Late Holocene.

270 The results of the proxies integral analysis have been linked to general climatic changes that

271 have occurred on a regional to global scale (Fig.3), and allow us to infer three major time
272 intervals, i.e., the MCA, the LIA and the current warm period (Mann et al. 2009), all of which
273 were characterized by changing continental versus marine influences in the study area.

274 The oldest recorded period, from 800 to 1300 AD, is closely associated with the MCA (reported
275 as a positive temperature anomaly in the northern hemisphere, Bradley et al., 2008; Mann et al.,
276 2009). During this period, a strong and steady influence of marine conditions governed the inner
277 Uruguayan continental shelf (inferred by low values of Ti/Ca and Fe/Ca, and a dominance of the
278 M-B diatom salinity group), probably as a result of a weakened RdIP water and terrigenous
279 sediment discharge. This situation led to a major **and more constant** sedimentation of marine
280 particulate carbon during the MCA (Perez et al., in press). In addition, the low Fe/K values
281 registered during the MCA would suggest conditions of reduced RdIP river discharge and dry
282 conditions over the drainage basin (Vuille et al., 2012). **Climatically drier conditions appear to**
283 **decrease chemical weathering in the Fe-rich RdIP drainage basin, thus depleting the Fe content**
284 **in the offshore depocenters in relation to K, which is associated with drier conditions (Depetris et**
285 **al., 2003; Depetris and Pasquini et al., 2007).**

286 Our findings, combined with those reported in other studies, suggest that a northward
287 displacement of the ITCZ and a weakened SAMS could have taken place during the MCA (Bird
288 et al., 2011a; Bird et al., 2011b; Vuille et al., 2012; Apaéstegui et al., 2014; Salvatecci et al.,
289 2014). **Though the continental SAMS exhibits spatial-temporal characteristics that differ from**
290 **the ITCZ, the latitudinal position of the ITCZ is closely related to changes in the SAMS**
291 **intensity, and both climatic elements also respond to temperature anomalies in the northern**
292 **hemisphere (Stríkis et al., 2011; Vuille et al., 2012).** In this sense, positive/negative northern
293 hemisphere temperature anomalies are linked to the north/south directional migration of the
294 ITCZ **thus diminishing/increasing SAMS activity** (Broccoli et al., 2006; Bird et al., 2011b;
295 **Stríkis et al., 2011; Vuille et al., 2012).** **Hence, the positive temperature anomalies in the**
296 **northern hemisphere during the MCA (Mann et al., 2009; probably associated with a positive**
297 **phase of the AMO), probably led to reduced SAMS and SACZ intensity, in addition to a**
298 **northward displacement of the ITCZ (Chiessi et al., 2009; Stríkis et al., 2011; Vuille et al.,**
299 **2012).** Such atmospheric conditions during the MCA led to a significant decrease in rainfall over
300 **the RdIP watershed (mainly in the catchment area of its main tributary, the Paraná River;**

301 Robertson and Mechoso, 2000). As a consequence of this, we inferred a reduction in both
302 freshwater and sediment input, in conjunction with an increase in salinity (Perez et al., in press)
303 on the Uruguayan continental shelf. The decrease in SACZ activity during the MCA could also
304 help explain the more humid conditions inferred for Uruguay during this episode (del Puerto et
305 al., 2013). This is associated with an increase in precipitation over the Uruguay River drainage
306 basins due to a reduced SACZ intensity as discuss below (Robertson and Mechoso, 2000).

307 The following period, from 1300 to 1850 AD, coincided with the LIA as reported for the
308 northern hemisphere (Bradley et al., 2003; Mann et al., 2009). This period is characterized by
309 higher values of Ti/Al, Fe/K, Ti/Ca and Fe/Ca than those recorded during the preceding period.
310 Therefore, we recorded a higher content of terrigenous material rich in Ti and Fe from the RdIP
311 watershed (Depetris et al., 2003; Depetris and Pasquini, 2007) which is associated with a higher
312 river discharge during the LIA (Fig. 4). Furthermore, a dominance of F diatoms (Fig. 3) was
313 detected. The F diatom group was mainly dominated by *Aulacoseira* spp., especially *A.*
314 *granulata* (Perez et al., in press), which is the most common diatom genus from the Paraná River
315 and the inner RdIP (Gomez and Bauer, 2002; Licursi et al., 2006; Devercelli et al., 2014).
316 Moreover, Massaferro et al. (2014) observed that the F diatom group recorded in the uppermost
317 55 cm of the sediment core GeoB 13813-4 was associated with the positive anomalies of the
318 Paraná River discharges. Thus, all the proxies indicate wetter conditions over the RdIP drainage
319 basin, and consequently, a major freshwater supply from the RdIP to the inner Uruguayan shelf
320 during the LIA. Accordingly, we observed the highest rates of terrigenous deposition during this
321 episode.

322 The LIA, characterized by cold conditions over the northern hemisphere, was then related to a
323 southward displacement of the ITCZ and a strengthening of SAMS and SACZ (Bird et al.,
324 2011b; Vuille et al., 2012). This leads to both a reduction in rainfall rates over northern South
325 America, Central America and Mexico (Haug et al., 2001; Vazques-Castro et al., 2008), and
326 elevated rainfall rates in the Andes (Sifeddine et al., 2008; Bird et al., 2011a; Bird et al., 2011b;
327 Vuille et al., 2012; Apaéstegui et al., 2014; Salvatecci et al., 2014), and over SESA (Meyer and
328 Wagner, 2009; Vuille et al., 2012). The intensification and northward displacement of the
329 Southern Westerlies during the LIA was also registered (Moy et al., 2009; Koffman et al., 2014).
330 This, in conjunction with a higher river discharge, would have also caused an anomalous

331 northward shift of the RdIP river plume. Such atmospheric conditions during the LIA have led to
332 a significant increase in rainfall over the RdIP watershed. Therefore, the outcome was a higher
333 influence of the RdIP river plume within the inner Uruguayan continental shelf as recorded in
334 this study.

335 The succession of maximum and minimum peaks in the element ratios from 1300 AD to present
336 (every 50 to 100 years), suggests an influence of the AMO on RdIP river discharge related to
337 changes in SAMS and SACZ intensity (Chiessi et al., 2009; Stríkis et al., 2011). The AMO
338 significantly affects the SAMS at multi-decadal time scales, leading to a reduced SAMS intensity
339 when the AMO is in its positive phase, and the ITCZ retreats northward, leading to a decrease in
340 RdIP river discharge (Chiessi et al., 2009; Strikis et al., 2011; Bird et al., 2011b). In addition,
341 Chiessi et al. (2009) proposed that sea surface temperature and atmospheric circulation
342 anomalies triggered by the AMO would control the variability in SAMS and SACZ intensity.

343 An increase in SACZ intensity during the LIA and its decrease during the MCA, inferred in this
344 study, explain the contrasting spatial/temporal climatic conditions recorded in the two regions in
345 the RdIP drainage basin (Vuille et al., 2012; del Puerto et al., 2013). SACZ intensity is associated
346 with increased river runoff in the northern region of the RdIP catchment area (Paraná River) and
347 a decreased runoff in the southern area (Uruguay River; Robertson and Mechoso, 2000). The
348 north/south river runoff contrast, in response to an intensified/weakened SACZ appear to
349 transport less/more moisture over the Uruguay River basin, thus leading to an increase/decrease
350 in precipitation during MCA/LIA over Uruguay (del Puerto et al., 2013).

351 Finally, the latest period started around 1850 AD, and is characterized by a sharp global increase
352 in temperature due to significant human impact (Crutzen, 2006; Halpern et al., 2008; Hoegh-
353 Guldberg and Bruno, 2010; Mauelshagen, 2014). Our sediment record for the last century
354 indicates a high river discharge as the highest element ratios were recorded, whilst the diatom
355 record shows a dominance of the M-B species, typical for marine-estuarine conditions. We make
356 the assumption that such a unique incongruence, compared with a optimal positive correlation
357 for the preceding time intervals, is not only a consequence of the regional anthropogenic impact
358 (Depetris and Pasquini, 2007; Bonachea et al., 2010, García-Rodríguez et al., 2010), as already
359 reported by Perez et al., (in press), but it is also related to natural changes associated with an

360 increasing Paraná river runoff after 1970 (Marrero et al., 2015).

361 **6 Conclusions**

362 The observed changes in the presented proxy records indicate variations in both the continental
363 runoff and the marine influence, related to regional climatic variability. Therefore, we put
364 forward the suggestion that global atmospheric changes (latitudinal shifts of the ITCZ, related to
365 changes in **SAMS and SACZ intensity**) have made an impact on the hydrodynamics and
366 consequently, on the local sedimentation regime, on the inner Uruguayan continental shelf over
367 the past 1200 cal yr BP (750-2000 AD).

368 During the MCA (800-1300 AD) a northward shift of the ITCZ **and a reduction in SAMS and**
369 **SACZ activities** would have caused a decrease in the rainfall rate over the RdIP drainage basin,
370 resulting in more estuarine-marine conditions predominating over a freshwater plume signal.
371 During the LIA (1400-1800 AD) in contrast, a southward shift of the ITCZ **and a strengthening**
372 **in SAMS and SACZ activities** led to an increased precipitation over the RdIP drainage basin,
373 reflected by stronger terrigenous influences in terms of freshwater supply on the inner
374 Uruguayan shelf. **Furthermore, a possible multi-decadal oscillation probably associated with**
375 **AMO since 1300 AD, reflects the variability in both the SASM and SACZ systems.**

376 **7 Acknowledgements**

377 We would like to express special thanks to Ines Sunesen, Eugenia Sar, M. Michel Mahiques and
378 Carina Lange for their fruitful discussions. We would also like to thank Vivienne Pettman for her
379 very valuable suggestions for improving the English **and also the reviewers for their critical**
380 **comments and suggestions which undoubtedly improved the manuscript content.** We
381 acknowledge PEDECIBA (Programa para el Desarrollo de las Ciencias Básicas) Geociencias,
382 ANII (Agencia Nacional de Investigación e Innovación), DAAD (German Academic Exchange
383 Service), and RLB (Red Latinoamericana de Botanica) for their financial support. **The authors**
384 **would also like to thank to PAGES for their partially financial support of this publication.** This
385 article is an outcome of the MARUM SD2 projectas part of the DFG 543 Research
386 Center/Excellence Cluster “The Ocean in the Earth System” at the University of Bremen.

387 **8 References**

388 Acha, E., Mianzan, H., Iribarne, O., Gagliardini, D., Lasta, C., and Daleo, P.: The role of
389 the Río de la Plata bottom salinity front in accumulating debris, *Mar. Poll. Bull.*, 46, 197-202,
390 2003.

391 Almeida, R. A. F., Nobre, P., Haarsma, R. J., and Campos, E. J. D.: Negative ocean-
392 atmosphere feedback in the South Atlantic Convergence Zone, *Geophys. Res. Lett.*, 34, L18809,
393 doi:10.1029/2007GL030401, 2007.

394 Apaéstegui, J., Cruz, F. W., Sifeddine, A., Vuille, M., Espinoza, J. C., Guyot, J. L.,
395 Khodri, M., Strikis, N., Santos, R. V., Cheng, H., Edwards, L., Carvalho, E., and Santini, W.:
396 Hydroclimate variability of the northwestern Amazon Basin near the Andean foothills of Peru
397 related to the South American Monsoon System during the last 1600 years, *Clim. Past.*, 10,
398 1967–1981, 2014.

399 Barreiro, M.: Influence of ENSO and the South Atlantic Ocean on climate predictability
400 over Southeastern South America, *Clim. Dyn.*, 35, 1493-1508, doi:10.1007/S00382-009-0666-9,
401 2010.

402 Bender, V. B., Hanebuth, T. J. J., and Chiessi, C. M.: Holocene shifts of the subtropical
403 shelf front off Southeastern South America controlled by high and low latitude atmospheric
404 forcings, *Paleoceanography*, 28, 1-10, doi: 10.1002/palo.20044, 2013.

405 Bird, B. W., Abbott, M. B., Rodbell, D. T., and Vuille, M.: Holocene tropical South
406 American hydroclimate revealed from a decadal resolved lake sediment $\delta^{18}\text{O}$ record, *Earth
407 Planet. Sc. Lett.*, 310, 192–202, 2011a.

408 Bird, B. W., Abbott, M. B., Vuille, M., Rodbell, D. T., Stansella, N. D., and
409 Rosenmeiera, M. F.: 2,300-year-long annually resolved record of the South American summer
410 monsoon from the Peruvian Andes, *PNAS*, 108, 8583–8588, 2011b.

411 Bisbal, G. A.: The southeast South American shelf large marine ecosystem: Evolution
412 and components, *Mar. Policy*, 19, 1, 21-38, 1995.

413 Blaauw, M., and Christen, J. A.: Flexible paleoclimate age-depth models using an
414 autoregressive gamma process, *Bay. Anal.*, 6, 457-474, 2011.

415 Bonachea, J., Bruschi, V. M., Hurtado, M. A., Forte, L. M., da Silva, R., Etcheverry, M.,
416 Cavallotto, J. L., Dantas, M. F., Pejon, O. J., Zuquette, L. Z., Bezerra, M. A. O., Remondo, J.,
417 Rivas, V., Gómez-Arozamena, J., Fernández, G., and Cendrero, A.: Natural and human forcing
418 in recent geomorphic change; case studies in the Rio de la Plata basin, *Sci. Total Environ.*, 408,
419 2674-2695, doi:10.1016/J.SCITOTENV.2010.03.00, 2010.

420 Bradley, R. S., Hughes, M. K., and Diaz, H. F.: Climate in Medieval Time, *Science*, 302,
421 404-405, 2008.

422 Broccoli, A. J., Dahl, K. A, and Stouffer, R. J.: Response of the ITCZ to Northern
423 Hemisphere cooling, *Geophys. Res. Lett.*, 33, L01702, doi:10.1029/2005GL024546, 2006.

424 Burone, L., Centurión, V., Cibils, L., Franco-Fraguas, P., García-Rodríguez, F., García,
425 G., and Pérez, L.: Sedimentología y Paleooceanografía, in: Programa oceanográfico de
426 caracterización del margen continental uruguayo-ZEE, edited by: Burone, L., Montevideo,
427 Uruguay, 240-295, 2012.

428 Burone, L., Ortega, L., Franco-Fraguas, P., Mahiques, M., García-Rodríguez, F.,
429 Venturini, N., Marin, Y., Brugnoli, E., Nagai, R., Muniz, P., Bicego, M., Figueira, R., and
430 Salaroli, A.: A multiproxy study between the Río de la Plata and the adjacent South-western
431 Atlantic inner shelf to asses the sediment footprint of river vs. marine influence, *Cont. shelf Res.*,
432 55, 141-154, 2013.

433 Camilloni, I.: Variabilidad y tendencias hidrológicas en la cuenca del Plata, in: El cambio
434 climático en el Río de la Plata, edited by: Barros, V., Menendez, A. and Nagy, G., CIMA,
435 Buenos Aires, 20-31, 2005.

436 Carvalho, L. M. V., Jones, C., and Liebmann, B.: The South Atlantic Convergence Zone:
437 Intensity, Form, Persistence, and Relationships with Intraseasonal to Interannual Activity and
438 Extreme Rainfall, *J. Climate*, 17, 88–108, 2004.

439 Chiessi, C. M., Mulitza, S., Patzold, J., Wefer, G., and Marengo, J. A.: Possible impact of
440 the Atlantic Multidecadal Oscillation on the South American summer monsoon. *Geophys. Res.*
441 *Lett.*, 36, L21707, doi:10.1029/2009GL039914, 2009.

442 Chiessi, C. M., Mulitza, S. G., Jeroen, S. J. B., Campos, M. C., and Gurgel, M. H. C.:
443 Variability of the Brazil Current during the late Holocene, *Palaeogeogr. Palaeocl.*, 415, 28–36,

444 doi: 10.1016/j.palaeo.2013.12.005, 2014.

445 Cioccale, M.: Climatic conditions in the central region of Argentina in the last 1000
446 years, *Quat. Int.*, 62, 35-47, 1999.

447 Ciotti, A. M., Odebrecht, C., Fillmann, G., and Moller, O. O.: Freshwater outflow and
448 Subtropical Convergence influence on phytoplankton biomass on the southern Brazilian
449 continental shelf, *Cont. Shel. Res.*, 15, 14, 1737-1756, 1995.

450 Crutzen, P. J.: The “Anthropocene”, in: *Earth System Science in the Anthropocene*,
451 edited by: Ehlers, E. and Krafft, T., Springer Berlin Heidelberg, 13-18, doi 10.1007/3-540-
452 26590-2, 2006.

453 del Puerto, L., García-Rodríguez, F., Bracco, R., Castiñeira, C., Blasi, A., Inda, H.,
454 Mazzeo, N. and Rodríguez, A.: Evolución climática holocénica para el sudeste de Uruguay,
455 Analisis multi-proxy en testigos de lagunas costeras, in: *El Holoceno en la zona costera de*
456 *Uruguay*, edited by: García-Rodríguez, F., Universidad de la Republica (UdelaR), 117-154,
457 2011.

458 del Puerto, L., Bracco, R., Inda, H., Gutierrez, O., Panario, D., and García-Rodríguez, F.:
459 Assessing links between late Holocene climate change and paleolimnological development of
460 Peña Lagoon using opal phytoliths, physical, and geochemical proxies, *Quat. Int.*, 287, 89-100,
461 doi:10.1016/j.quaint.2011.11.026, 2013.

462 Depetris, P.J. and Kempe, S.: The impact of the El Niño 1982 event on the Paraná River,
463 its discharge and carbon transport. *Palaeogeogr. Palaeoclimatol.*, 89, 239-244, 1990.

464 Depetris, P. J. and Pasquini, A. I.: Discharge trends and flow dynamics of southern
465 southamerican rivers draining the southern Atlantic seaboard: an overview, *J. Hydrol.*, 333, 385-
466 399, doi: 10.1016/j.hydrol.2006.09005, 2007.

467 Depetris, P. J., Probst, J-L., Pasquini, A. I. and Gaiero, D. M.: The geochemical
468 characteristics of the Paraná River suspended sediment load: an initial assessment, *Hydrol.*
469 *Process*, 17, 1267–1277, doi: 10.1002/hyp.1283, 2003.

470 Devercelli, M., Zalocar de Domitrovic, Y., Forastier, M. E. and Meichtry de Zaburlín N.:
471 Phytoplankton of the Paraná River Basin, *Advanc. Limnol.*, 65, 39–65, doi: 10.1127/1612-

472 166X/2014/0065-0033, 2014.

473 Francus, P., Lamb, H., Nakawaga, T., Marshall, M., and Brown, E.: The potential of high
474 resolution X-ray fluorescence core scanning: Applications in paleolimnology, *PAGES news* 17, 9,
475 93-95, 2009.

476 Frenguelli, J.: Diatomeas del Río de la Plata, *Revista Museo Nacional La Plata*, III, 213-
477 334, 1941.

478 Frenguelli, J.: Diatomeas del Platense, *Revista Museo Nacional La Plata*, III, 77-221,
479 1945.

480 FREPLATA: Análisis Diagnóstico Transfronterizo del Río de la Plata y su Frente
481 Marítimo. Documento Técnico. Proyecto “Protección Ambiental del Río de la Plata y su Frente
482 Marítimo: Prevención y Control de la Contaminación y Restauración de Hábitats”. Proyecto
483 PNUD/GEF/RLA/99/G31, 106, 2004.

484 Garcia, S. and Kayano, M.: Some evidence on the relationship between the South
485 American monsoon and the Atlantic ITCZ, *Theor. Appl. Climatol.*, 99, 29–38, 2010.

486 García-Rodríguez, F., Hutton, M., Brugnoli, E., Venturini, N., del Puerto, L., Inda, H.,
487 Bracco, R., Burone, L., and Muniz, P.: Assessing the effect of natural variability and human
488 impacts on the environmental quality of a coastal metropolitan area (Montevideo Bay, Uruguay),
489 *PANAMJAS*, 5, 1, 90–99, 2010.

490 García-Rodríguez, F., Brugnoli, E., Muniz, P., Venturini, N., Burone, L., Hutton, M.,
491 Rodríguez, M., Pita, A., Kandravicius, N., Perez, L., and Verocai, J.: Warm-phase ENSO
492 events modulate the continental freshwater input and the trophic state of sediments in a large
493 South American estuary. *Mar. Freshwater Res.*, 65, 1-11, 2014.

494 Garreaud, R. D., Vuille, M., Compagnucci, R., and Marengo, J.: Present-day South
495 American climate, *Palaeogeogr. Palaeoclimatol.*, 281, 3-4, 180-195, 2009.

496 Giberto, D. A., Bremec, C. S., Acha, E. M., and Mianzan, H.: Large-scale spatial patterns
497 of benthic assemblages in the SW Atlantic: the Río de la Plata, *Estuar. Coast. Shelf S.*, 61, 1-13,
498 2004.

499 Goldberg, E. D., and Arrhenius, G.O.S.: *Geochemistry of pacific pelagic sediments,*

500 **Geochim. Cosmochim. Ac., 13, 153-212, 1958.**

501 Gómez, N. and Bauer, D. E.: Diversidad fitoplanctónica en la franja costera Sur del Río
502 de la Plata, *Biol. Acuát.*, 19, 7-26, 2000.

503 González-Mora, B. and Sierro, F. J.: Caracterización geoquímica de las capas ricas en
504 materia orgánica registradas durante el estadio isotópico marino 7 en el Mar de Alborán
505 (Mediterráneo occidental), *GEOGACETA*, 43, 111-114, 2007.

506 Govin, A., Holzwarth, U., Heslop, D., Ford Keeling, L., Zabel, M., Mulitza, S., Collins, J.
507 A., and Chiessi, C. M.: Distribution of major elements in Atlantic surface sediments (36°N–
508 49°S): Imprint of terrigenous input and continental weathering, *Geochem. Geophys. Geosys*, 13,
509 1, 1525-2027, 2012.

510 Guerrero, R., Acha, E., Framiñan, M., and Lasta, C.: Physical oceanography of the Rio de
511 la Plata Estuary, Argentina, *Cont. Shelf. Res.*, 17, 7, 727-742, 1997.

512 Haberzettl, T., Fey, M., Lucke, A., Maidana, N., Mayr, C., Ohlendorf, C., Schabitz, F.,
513 Schleser, G. H., Wille, M. and Zolitschka, B.: Climatically induced lake level changes during the
514 last two millennia as reflected in sediments of Laguna Potrok Aike, southern Patagonia (Santa
515 Cruz, Argentina), *J. Paleolimnol.*, 33, 283–302, 2005.

516 Halpern, B. S., Walbridge, S., Selkoe, K. A., Kappel, C. V., Micheli, F., D'Agrosa, C.,
517 Bruno, J. F., Casey, K. S., Ebert, C., Fox, H. E., Fujita, R., Heinemann, D., Lenihan, H., Madin,
518 E. M., Perry, M. T., Selig, E., Spalding, M., Steneck, R. and Watson, R.: A Global Map of
519 Human Impact on Marine Ecosystems, *Science*, 319, 948-951, 2008.

520 Hanebuth, T. J. J., Lantzsch, H., García-Rodríguez, F. and Perez, L.: Currents controlling
521 sedimentation: paleo-hydrodynamic variability inferred from the continental-shelf system off SE
522 South America (Uruguay), in: *Ciencias Marino Costeras en el Umbral del Siglo XXI: Desafíos*
523 *en Latinoamérica y el Caribe (XV COLACMAR)*, edited by: Muniz, P., Conde, D., Venturini, N.
524 and Brugnoli, E., in press.

525 Hasle, G. R. and Syvertsen, E. E.: Marine diatoms, in: *Identifying marine phytoplankton*,
526 edited by: Tomas, C. R., Academic Press, San Diego, California, 5-385, 1996.

527 Hassan, G.: Paleocological significance of diatoms in argentinean estuaries, Consejo

528 Nacional de Investigaciones Científicas y Técnicas (CONICET), Argentina, 2010.

529 Haug, G. H., Hughen, K. A., Sigman, D. M., Peterson, L. C. and Rohl, U.: Southward
530 Migration of the Intertropical Convergence Zone Through the Holocene, *Science*, 293, 1304-
531 1307, doi: 10.1126/science.1059725, 2001.

532 Hoegh-Guldberg, O., and Bruno, J. F.: The Impact of Climate Change on the World's
533 Marine Ecosystems, *Science*, 328, 1523-1528, doi: 10.1126/science.1189930, 2010.

534 Iriondo, M.: Climatic changes in the South American plains: Records of a continent-scale
535 oscillation, *Quatern. Int.*, 57-58, 93-112, 1999.

536 Jansen, J. H. F., Van der Gaast, S. J., Koster, B., and Vaars A. J.: CORTEX, a shipboard
537 XRF-scanner for element analyses in split sediment cores, *Mar. Geol.*, 151, 1-4, 143-153,
538 doi:10.1016/S0025 3227(98)00074-7, 1998.

539 Koffman, B. G., Kreutz, K. J., Breton, D. J., Kanel, E. J., Winski, D. A., Birkel, S. D.,
540 Kurbatov, A. V., and Handley, M. J.: Centennial-scale variability of the Southern Hemisphere
541 westerly wind belt in the eastern Pacific over the past two millennia, *Clim. Past*, 10, 1125-1144,
542 doi:10.5194/cp-10-1125-2014, 2014.

543 Krastel, S., Wefer, G., Hanebuth, T. J. J., Antobreh, A. A., Freudenthal, T., Preu, B.,
544 Schwenk, T., Strasser, M., Violante, R., and Winkelmann, D.: Sediment dynamics and
545 geohazards off Uruguay and the de la Plata River region (northern Argentina and Uruguay),
546 *Geo-Mar. Let.*, 31, 4, 271-283, doi: 10.1007/s00367-011-0232-4, 2011.

547 Krastel, S., Wefer, G. and cruise participants: Sediment transport off Uruguay and
548 Argentina: From the shelf to the deep sea. 19.05.2009 – 06.07.2009, Montevideo (Uruguay) –
549 Montevideo (Uruguay), Report and preliminary results of RV METEOR Cruise M78/3, *Berichte*,
550 *Fachbereich Geowissenschaften, Universität Bremen*, 285, 2012.

551 Lantsch, H., Hanebuth, T. J. J., Chiessi, C. M., Schwenk, T., and Violante, R.: A high-
552 supply sedimentary system controlled by strong hydrodynamic conditions (the continental
553 margin off the Plata Estuary during the late Quaternary, *Quat. Res.*, 81, 2, 339-354, 2014.

554 Licursi, M., Sierra, M. V., and Gómez, N.: Diatom assemblages from a turbid coastal
555 plain estuary: Río de la Plata (South America), *J. Marine Syst.*, 62, 33-45, 2006.

556 Löwemark, C., Chen, H., Yang, T-N., Kylander, M., Yu, E-F., Hsu, Y-W., Lee, T-Q.,
557 Song, S-R., and Jarvis, S.: Normalizing XRF scanner data: A cautionary note on the
558 interpretation of high-resolution records from organic-rich lakes, *J. Asia Earth Sci.*, 40, 1250-
559 1256, 2011.

560 Mahiques, M. M., Wainer, I. K. C., Burone, L., Nagai, R., Sousa, S. H. M., Lopes
561 Figueira, R. C., da Silveira, I. C. A., Bicego, M. C., Alves, D. P. V., and Hammer, O.: A high-
562 resolution Holocene record on the Southern Brazilian shelf: Paleoenvironmental implications,
563 *Quatern. Int.*, 206, 52-61, 2009.

564 Mahowald, N. M., Muhs, D. R., Levis, S., Rasch, P. J., Yoshioka, M., Zender, C. S., and
565 Luo, C.: Change in atmospheric mineral aerosols in response to climate: Last glacial period,
566 preindustrial, modern, and doubled carbon dioxide climates, *J. Geophys. Res.*, 111, D10202,
567 doi:10.1029/2005JD006653, 2006.

568 Mann, M. E., Zhang, Z., Rutherford, S., Bradley, R. S., Hughes, M., Shindell, D.,
569 Ammann, D., Faluvegi, G., and Ni, F.: Global Signatures and Dynamical Origins of the Little Ice
570 Age and Medieval Climate Anomaly, *Science*, 326, 1256-1259, 2009.

571 Marrero, A., Tudurí, A., Perez, L., Cuña, C., Muniz, P., Lopes Figueira, C. R., Mahiques,
572 M. M., Pittauerová, D., Hanebuth, T. J. J., and García- Rodríguez, F.: Cambios históricos en el
573 aporte terrígeno de la cuenca del Río de la Plata sobre la plataforma interna uruguaya, *LAJSBA*,
574 21, 2, 165-179, 2015.

575 Martins, V., Dubert, J., Jouanneau, J.-M., Weber, O., Ferreira da Silva, E., Patinha, C.,
576 Alverinho Dias, J.M., and Rocha, F.: A multiproxy approach of the Holocene evolution of shelf-
577 slope circulation on the NW Iberian continental shelf, *Mar. Geol.*, 239, 1–18, 2007.

578 Martins, L. R., Martins, I. R., and Urien, C. M.: Aspectos sedimentares da plataforma
579 continental na área de influencia de Rio de La Plata, *Gravel*, 1, 68-80, 2003.

580 Martins, L. R. and Urien, C. R.: Areias da plataforma e a erosao costeira, *Gravel*, 2, 4-24,
581 2004.

582 Masello, A. and Menafra, R.: Macrobenthic communities of the Uruguayan coastal zona
583 and adjacent areas, in: *Río de la Plata una revisión ambiental*, edited by: Wells, P. G. and
584 Daborn, G. R., University of Dalhousie, 140-186, 1998.

585 Massafarro, J., Perez, L., de Porras, M. E., Pérez Becoña, L., Tonello, M., and Juggins,
586 S.: Paleocological data analysis with R, course for Latin American researchers, Pages
587 Magazine, Workshop reports, 22 , 2, 105, 2014.

588 Mauelshagen, F.: Redefining historical climatology in the Anthropocene. The
589 Anthropocene Review, 1, 2, 171-204, doi: 10.1177/2053019614536145, 2014.

590 Metzeltin, D. and García-Rodríguez, F. (Eds): Las Diatomeas Uruguayas, Facultad de
591 Ciencias, Montevideo, Uruguay, 654, 2003.

592 Metzeltin, D., Lange-Bertalot, H. and García-Rodríguez, F. Diatoms of Uruguay -
593 Taxonomy, Biogeography, Diversity, in: Iconographia Diatomologica (15), edited by: Lange-
594 Bertalot, H. and Gantner Verlag, A. R. G., Koenigstein, Germany, 736, 2005.

595 Meyer, I. and Wagner, I.: The Little Ice Age in Southern South America: Proxy and
596 model based evidence, in: Past climate variability in South America and surrounding regions,
597 from the last glacial maximum to the Holocene, edited by: Vimeux, F., Sylvestre, F. and Khodri,
598 M., Springer, 395-412, 2009.

599 Möller, Jr. O. O., Piola, A. R., Freitas, A. C., and Campos, E.: The effects of river
600 discharge and seasonal winds on the shelf off southeastern South America, Cont. Shelf Res., 28,
601 13, 1603-1624, 2008.

602 Moy, C. M., Moreno, P. I., Dunbar, R. B., Kaplan, M. R., Francois, J-P., Villalba, R., and
603 Haberzettl, T.: Climate change in Southern South America during the last two millennia, in: Past
604 climate variability in South America and surrounding regions, edited by: Vimeux, F., Sylvestre,
605 F. and Khodri, M., Developments in Paleoenvironmental Research (14), Springer, 353-393,
606 2009.

607 Müller-Melchers, P.: Diatomeas procedentes de algunas muestras de turba del Uruguay.
608 Comunicaciones Botánicas del Museo de Historia Natural de Montevideo, 1, 17, 1-25, 1945.

609 Müller-Melchers, P.: Sobre algunas diatomeas planctónicas de Atlántida (Uruguay),
610 Physis, 20, 59, 459-466, 1953.

611 Müller-Melchers, P.: Plankton diatoms of the Southern Atlantic of Argentina and
612 Uruguay coast. Comunicaciones Botánicas del Museo de Historia Natural de Montevideo 3, 38,

613 1-53, 1959.

614 Nagai, R. H., Ferreira, P. A. L., Mulkherjee, S., Martins, V. M., Figueira, R. C. L., Sousa,
615 S. H. M. and Mahiques, M. M.: Hidrodinamic controls on the distribution of surface sediments
616 from the southeast South American continental shelf between 23 S and 38 S, *Cont. Shelf. Res.*,
617 89, 51-60, doi.org/10.1016/j.csr.2013.09.016, 2014.

618 Nogués-Paegle, J., Mechoso, C. R., Fu, R., Berbery, E. H., Chao, W. C., Chen, T.-C.,
619 Cook, K., Diaz, A. F., Enfield, D., Ferreira, R., Grimm, A. M., Kousky, V., Liebmann, B.,
620 Marengo, J., Mo, K., Neelin, J. D., Paegle, J., Robertson, A. W., Seth, A., Vera, C. S., and Zhou,
621 J.: Progress in Pan American CLIVAR research: Understanding the South American monsoon.
622 *Meteorologica*, 27, 3-32, 2002.

623 Perez, L., García-Rodríguez, F., and Hanebuth, T.: Paleosalinity changes in the Río de la
624 Plata estuary and on the adjacent Uruguayan continental shelf over the past 1200 cal ka BP: an
625 approach using diatoms as proxy, in: Applications of paleoenvironmental techniques in estuarine
626 studies, *Developments in Paleoenvironmental Research (DPER)*, edited by: Weckström, K.,
627 Saunders, P. and Skilbeck, G., Springer, in press.

628 Piola, A. R., Campos, E. J. D., Möller Jr., O. O., Charo, M., and Martinez C. M.:
629 Subtropical shelf front off eastern South America, *J. Geophys. Res.*, 105, 6566–6578, 2000.

630 Piola, A. R., Moller, O. O., Guerrero, R. A. and Campos, E. J. D.: Variability of the
631 subtropical shelf front off eastern South America: Winter 2003 and summer 2004, *Cont. Shelf*
632 *Res.*, 28, 1639-1648, doi: 10.1016/j.csr.2008.03.013, 2008.

633 Piovano, E. L., Ariztegui, D., Cordoba, F., Cioccale, J. and Sylvestre, F.: Hydrological
634 variability in South America below the tropic of Capricorn (Pampas and Patagonia, Argentina)
635 during the Last 13.0 Ka, in: Past climate variability in South America and surrounding regions,
636 from the last glacial maximum to the Holocene, edited by: Vimeux, F., Sylvestre, F. and Khodri,
637 M., Springer, 323-352, 2009.

638 Razik, S., Chiessi, C. M, Romero, O. E. and von Dobeneck, T.: Interaction of the South
639 American Monsoon System and the Southern Westerly Wind Belt during the last 14 kyr
640 *Palaeogeogr. Palaeocl.*, 374, 28–40, 2013.

641 Reimer, P.J., Bard, E., Bayliss, A., Beck, J.W., Blackwell, P.G., Bronk Ramsey, C.,

642 Buck, C.E., Edwards, R.L., Friedrich, M., Grootes, P.M., Guilderson, T.P., Haflidason, H.,
643 Hajdas, I., Hatté, C., Heaton, T.J., Hoffmann, D.L., Hogg, A.G., Hughen, K.A., Kaiser, K.F.,
644 Kromer, B., Manning, S.W., Niu, M., Reimer, R.W., Richards, D.A., Scott, M.E., Southon, J.R.,
645 Turney, C.S.M., and van der Plicht, J.: IntCal13 and Marine13 radiocarbon age calibration
646 curves 0-50,000 yr cal BP, *Radiocarbon*, 55, 4, 1869-1887, 2013.

647 Robertson, A. W., and Mechoso, C. R.: Interannual and interdecadal variability of the
648 South Atlantic Convergence Zone. *Mon. Wea. Rev.*, 128, 2947-2957, 2000.

649 Romero, O. E., Lange, C. B., Fischer, G., Treppke, U. F., and Wefer, G.: Variability in
650 export production documented by downward fluxes and species composition of marine panctonic
651 diatoms: Observations from the tropical and ecuatorial Atlantic, in: Use of proxies in
652 paleoceanography: Examples from the South Atlantic, edited by: Fischer, G. and Wefer, G.,
653 Universitat Bremen, Springer, Germany, 365–392, 1999.

654 Salazar, A., Lizano, O. G. and Alfaro, E. J.: Composición de sedimentos en las zonas
655 costeras de Costa Rica utilizando Fluorescencia de Rayos-X (FRX), *Rev. biol. Trop.*, 52, 2,
656 2004.

657 Salvattecí, R., Gutiérrez, D., Field, D. and Sifeddine, D., Ortlieb, L., Bouloubassi, I.,
658 Boussafir, M., Boucher, H and Cetin, F.: The response of the Peruvian Upwelling Ecosystem to
659 centennial-scale global change during the last two millennia, *Clim. Past*, 10, 715–731,
660 doi:10.5194/cp-10-715-2014, 2014.

661 Sar, E. A., Sunesen, I. and Lavigne, A. S.: *Cymatotheca*, *Tryblioptychus*, *Skeletonema*
662 and *Cyclotella* (Thalassiosirales) from Argentinian coastal waters. Description of *Cyclotella*
663 *cubiculata* sp. nov., *Vie milieu*, 60, 2, 135-156, 2010.

664 Sifeddine, A., Gutiérrez, D., Ortlieb, L., Boucher, H., Velazco, F., Field, D., Vargas, G.,
665 Boussafire, M., Salvattecí, R., Ferreira, V., García, M., Valdés, J., Caquineau, S., Mandeng
666 Yogo, M., Cetin, F., Solis, J., Soler, P. and Baumgartner, T.: Laminated sediments from the
667 central Peruvian continental slope: A 500 year record of upwelling system productivity,
668 terrestrial runoff and redox conditions, *Prog. Oceanog.*, 79, 2-4, 190-197, 2008.

669 Strikis, N. M., Cruz Jr., F. W., Cheng, H., Karmann, I., Edwards, R. L., Vuille, M.,
670 Wang, X., de Paula, M. S., Novello, V. F., and Auler, A. S.: Abrupt variations in South

671 American monsoon rainfall during the Holocene based on a speleothem record from central-
672 eastern Brazil, *Geology*, 39, 1075–1078, 2011.

673 Urien, C. M., and Ewing, M.: Recent sediments and environment of southern Brazil,
674 Uruguay, Buenos Aires, and Rio Negro continental shelf, in: *The Geology of Continental*
675 *Margins*, edited by: Burk, C. A., and Drake, C. L., Springer, New York, 157-177, 1974.

676 Urien, C. M., Martins, L. R., and Martins, I. R.: Evolução geológica do Quaternário do
677 litoral atlântico uruguaio, plataforma continental e regiões vizinhas, *Notas Técnicas,*
678 *CECO/URFGS*, 3, 7-43, 1980.

679 Vázquez-Castro, G., Ortega-Guerrero, B., Rodríguez, A., Caballero, M., and Lozano-
680 García, S.: Mineralogía magnética como indicador de sequía en los sedimentos lacustres de los
681 últimos *ca.* 2,600 años de Santa María del Oro, occidente de México, *Rev. Mex. Cienc. Geol.*,
682 25, 1, 21-38, 2008.

683 Vuille, M., Burns, S. J., Taylor, B. L., Cruz, F. W., Bird, B.W., Abbott, M. B., Kanner, L.
684 C., Cheng, H., and Novello V. F.: A review of the South American monsoon history as recorded
685 in stable isotopic proxies over the past two millennia, *Clim. Past.*, 8, 1309–1321, doi:10.5194/cp-
686 8-1309-2012, 2012.

687 Weltje, G. J., and Tjallingii, R.: Calibration of XRF core scanners for quantitative
688 geochemical logging of sediment cores: Theory and application, *Earth Planet. Sci. Lett.*, 274, 3–
689 4, 423–438. doi:10.1016/j.epsl.2008.07.054, 2008.

690 Witkowski, A., Lange-Bertalot, H., and Metzeltin, D.: Diatom flora of marine coasts 1,
691 in: *Iconographia Diatomologica*, edited by: Lange-Bertalot, H., and Gantner Verlag A.R.G., 7,
692 925, 2000.

693 Yarincik, K., Murray, M., R. W., and Peterson, L. C: Climatically sensitive eolian and
694 hemipelagic deposition in the Cariaco Basin, Venezuela, over the past 578,000 years: Results
695 from Al/Ti and K/Al, *Paleoceanography*, 15, 2, 210–228, doi:10.1029/1999PA900048, 2000.

696 Zhou, J. and Lau, K.-M.: Does a monsoon climate exist over South America?, *J. Climate*,
697 11, 1020–1040, 1998.

698

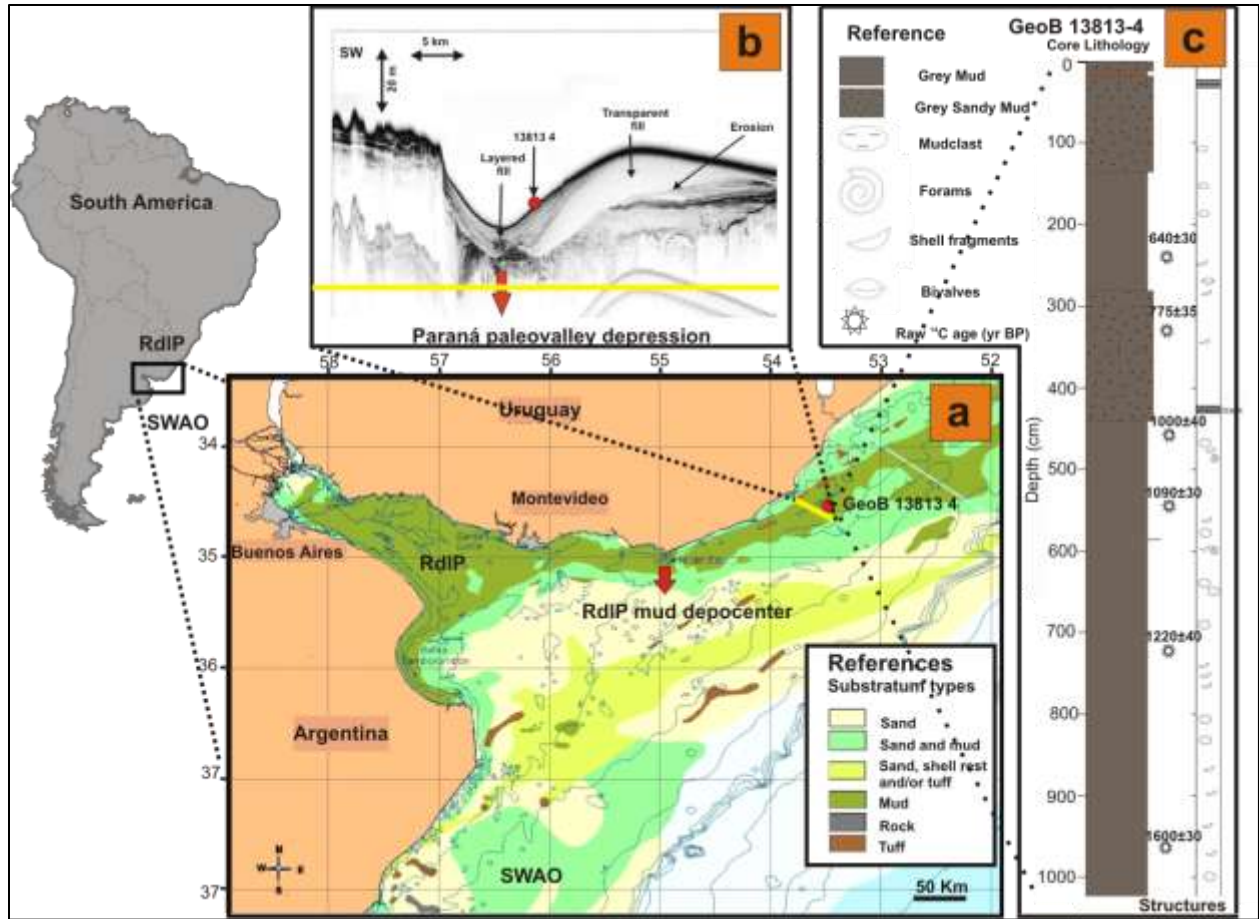
699

Table 1. Radiocarbon dates as obtained from the Bacon modeling.

Lab # (Poz-)	Depth in core (cm)	Raw ¹⁴C age (yr BP)	Bacon weighted average age (cal yr BP)	Bacon weighted average age (cal yr AD)	Sedimentation rate (cm yr⁻¹)
35198	255	640± 30	230	1688	0.72
47935	305	775± 35	371	1494	0.68
42428	447	1000± 40	552	1293	0.78
35199	560	1090± 30	665	1167	1.00
47937	705	1220± 40	830	994	0.88
42429	964	1600± 30	1197	753	0.70

700

701



702

703 **Fig.1. (a)** Study area: The red circle indicates the location of Core GeoB 13813-4 retrieved from
 704 the inner-shelf mud depocenter off the Uruguayan coast (modified from Freplata, 2004). **(b)** Rio
 705 de la Plata (RdIP) mud depocenter (PARASOUND sub-bottom profile), which represents the RdIP
 706 paleo-valley and its sedimentary multi-story filling succession. **(c)** GeoB 13813-4 core lithology.
 707 (1b and 1c modified from Krastel et al., 2012 and Lantzsch et al., 2014). Stars on the right of the
 708 sediment core indicate ¹⁴C-dated intervals.

709

710

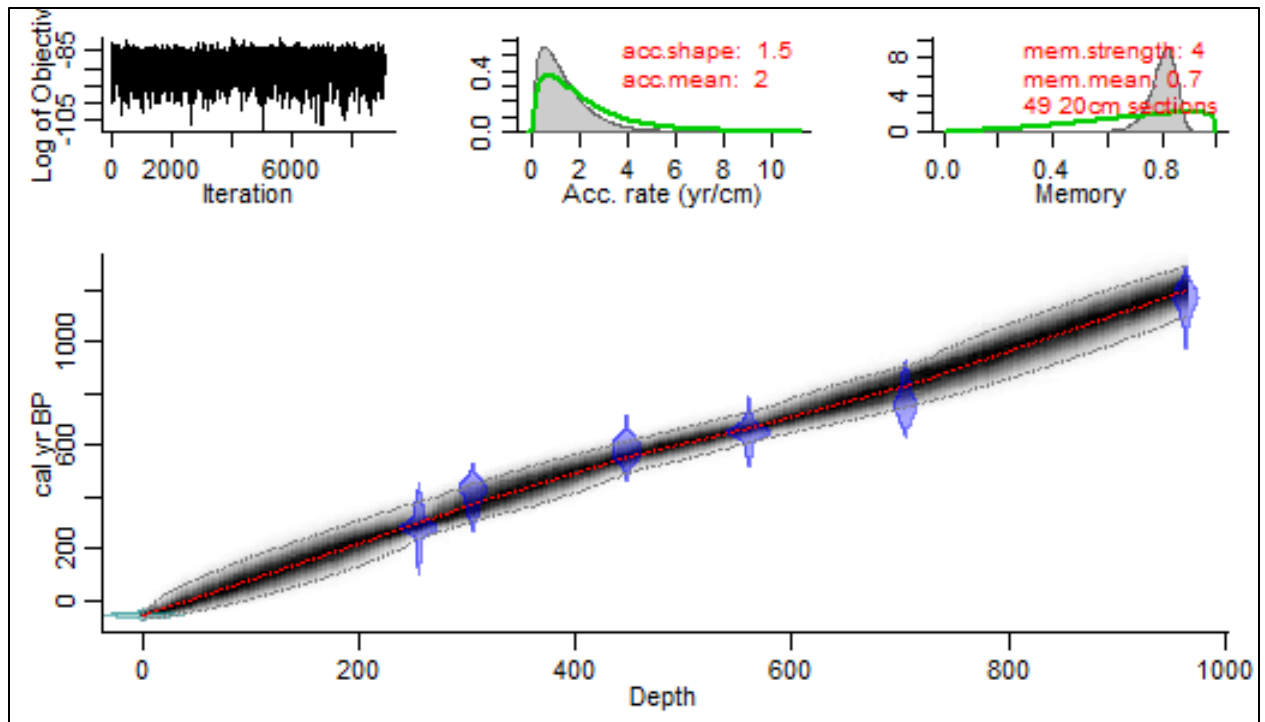
711

712

713

714

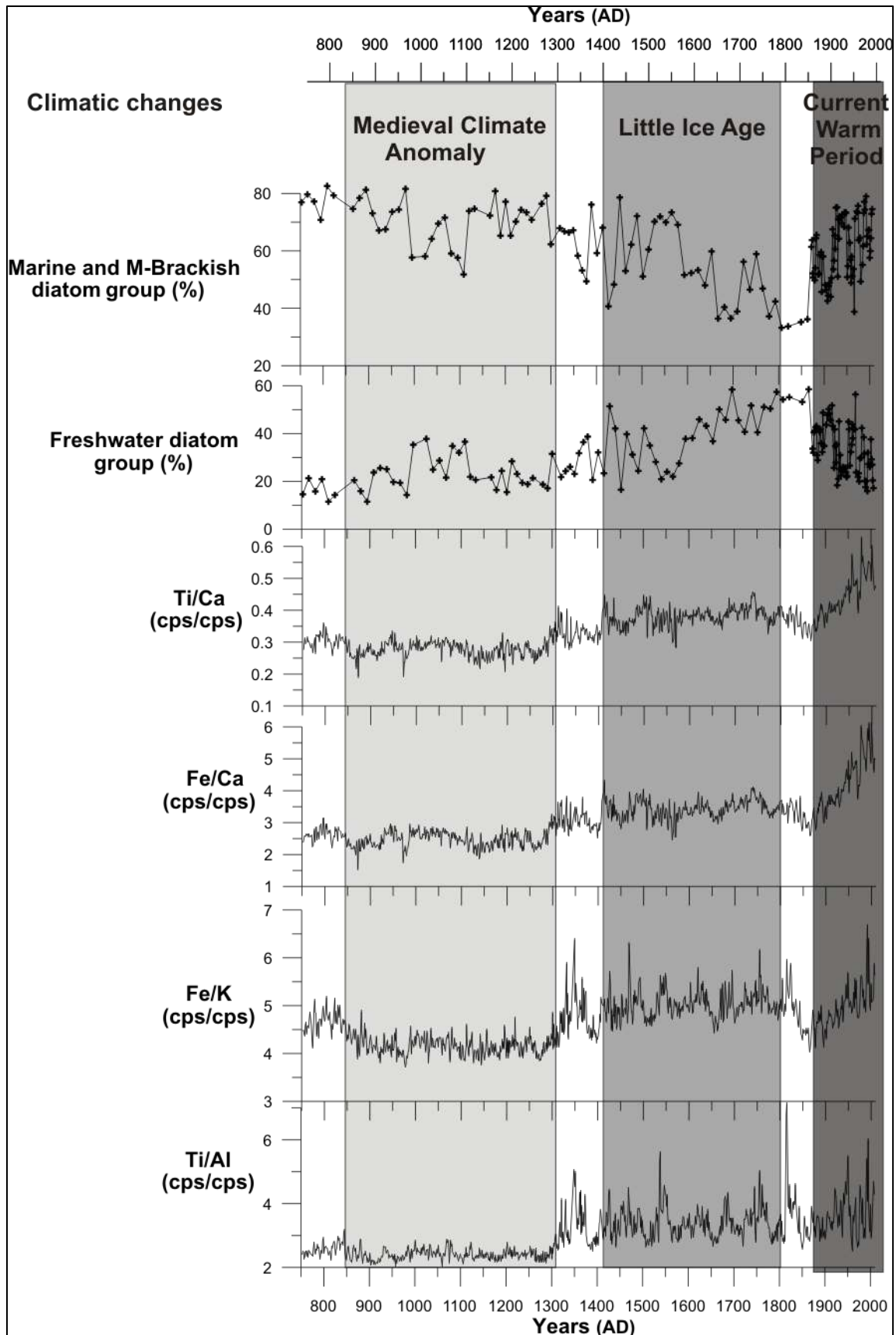
715



716

717 **Fig. 2.** The age-depth model for core GeoB 13813-4 using the program Bacon. Upper panels
 718 depict the Markov Chain Monte Carlo (MCMC) iterations (left), the prior (green curves) and
 719 posterior (grey histograms) distributions for the sedimentation rate (middle panel) and memory
 720 (right panel). The bottom panel shows the calibrated ^{14}C dates (transparent blue), extraction year
 721 of the core (-59 yr BP, 2009 AD, transparent blue light) and the age-depth model (grey stippled
 722 lines indicate the 95 % confidence intervals; the red curve shows the 'best' fit based on the
 723 weighted mean age for each depth).

724



726 **Fig. 3.** Centennial variation of Ti/Al, Fe/K, Ti/Ca, Fe/Ca ratios, and the freshwater and marine,
727 marine-brackish salinity-indicative diatom groups from the sediment core GeoB 13813-4 (from
728 bottom to top, respectively), during the last 1200 yr BP (750-2000 cal yr AD). The major
729 climatic changes during this period of time were the Medieval Climatic Anomaly and the Little
730 Ice Age.

731